Generation of Human Walking Paths

Alessandro Vittorio Papadopoulos, Luca Bascetta, and Gianni Ferretti

Abstract— This work investigates the way humans plan their paths in a goal-directed motion. The person can be viewed as an optimal controller that plans the path minimizing a certain (unknown) cost function. Taking this viewpoint, the problem can be formulated as an inverse optimal control one, i.e., starting from control and state trajectories we want to figure out the cost function used by a person while planning the path. To test the envisaged ideas, a set of walking paths of different volunteers were recorded using a motion capture facility. The collected data have been used to compare a solution to the inverse control problem coming from the literature to a novel one. The obtained results, ranked using the discrete Fréchet distance, show the effectiveness of the proposed approach.

I. Introduction

Despite the impressive achievements of robotics research during the last decade, the use of robots in industrial applications that need a physical interaction with humans is still severely limited by safety issues. In particular, allowing humans working side by side with industrial robots is still far from being a common industrial practice. To achieve this goal the control system should be able to prevent dangerous situations, by estimating the human intention in time to perform a safe robot reaction.

While the estimation of the human intention [1] quite a hard problem, in the case of walking of a human being one can predict her/his trajectory in a goal-oriented motion [2], based on a model of the way a human plans the path.

One of the most recent and promising approaches to deal with the prediction of goal-oriented motion models the human planning as an optimal control problem whose cost function, however, is unknown. As a consequence, the problem of predicting where a human is heading to can be converted into an inverse optimal control problem.

The inverse problem has been a widely studied problem [3], [4], and has a variety of applications both inside and outside the field of robotics. In the context of planning human walking paths, it has been used many times with various approaches. In [2] and [5] the authors assume that decisions are optimal w.r.t. a certain (unknown) cost function, and try to minimize the difference between what is observed and what would have been observed given a candidate cost function. The cost function is represented as a linear combination of basis functions weighted by an unknown parameter vector. Their approach infers the parameter vector, solves the corresponding optimal control problem, predicts what the resulting observations would be, and then applies

derivative-free optimization to minimize the difference between predicted and observed trajectories. This approach, however, is computationally expensive as it requires solving an optimal control problem at each iteration of the optimizer.

Another approach is presented in [6], in which the authors implement several algorithms, based on inverse reinforcement learning, that do not require solving the forward problem.

The method proposed herein is inspired by [7], [8]. This new formulation of inverse optimal control assumes that the observations are perfect, while the system is considered to be only approximately optimal. This allows to define residual functions based on the Karush-Kuhn-Tucker (KKT) necessary conditions for optimality [9]. Then, the inverse optimal control problem can be solved by minimizing these residual functions, recovering the parameters that govern the cost function. As a result, the inverse optimal control problem reduces to a simple least-squares minimization, which can be solved very efficiently.

The present paper extends the work in [7], [8], trying to overcome some of the limitations that arise applying those approach to our dataset. To be more specific, in this paper the walking paths instead of the walking trajectories are considered, expressing the motion model with respect to the natural coordinate so that it is invariant to walking velocity changes. Further, a novel cost function, that considers the energy and the position of the human with respect to the target as well, is introduced. Finally, the discrete Fréchet distance is proposed as a tool to assess the similarity of a set of paths.

The paper is organized as follows. In Section II a detailed description of the experiments performed to collect the data is provided. Section III describes how the inverse optimal control problem is solved and a comparison with respect to a previous approach is reported. Section IV shows and discusses the results obtained with the proposed approach. Section V presents the future research and concludes the manuscript.

II. Experimental setup

In this section we describe the experimental setup used to collect a dataset of human walking paths. About one thousand paths were recorded using a 6 cameras motion capture system (SMART system by BTS S.p.A.). Each subject was equipped with 3 light reflective markers, two located on the hips – anterior superior iliac spine (asis) –, and one located on the sacrum (see Fig. 1).

The experimental protocol was inspired to the one adopted in [5]. More specifically, we restrict the study to the "natural" forward locomotion, excluding goals located behind the starting position and goals requiring side-walk steps.
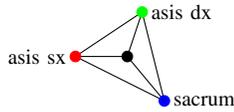Goals are defined both in position and orientation, and in

Fig. 1: Marker positions and barycentre.

order to cover at best the accessibility region, the space for the experiments, a 4m×6m rectangle corresponding to the calibrated volume, was sampled with 144 points defined by 12 positions on a 2D grid and 12 orientations each. The final orientation varied from 0 to 2π in intervals of $\pi/6$ at each final position (see Fig. 2). The starting position was always the same.
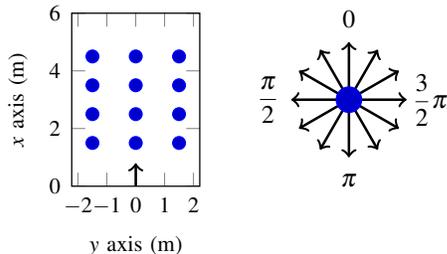

Fig. 2: Final porch positions (left) and orientations (right).

Locomotor trajectories of seven normal healthy people (both males and females), who volunteered for participation in the experiments, were recorded. Their ages, heights, and weights ranged from 24 to 50 years, from 1.60 to 1.85m, and from 50 to 90kg, respectively.

Each subject performed all the 144 trajectories. Subjects walked from the same initial configuration to a randomly selected final configuration (see Fig. 2). The target consisted of a porch that could be rotated around a fixed position in order to show the desired final orientation (see Fig. 3).

The subjects were instructed to freely cross over this porch without any spatial constraint relative to the path they might take. Further, they were allowed to choose their natural walking speed to perform the task.
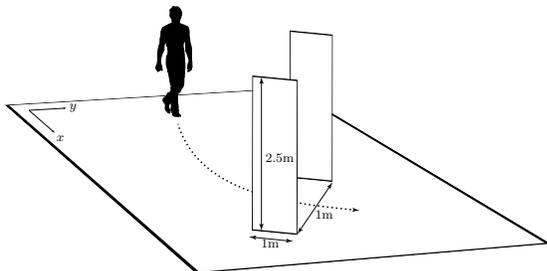

Fig. 3: An example of experiment.

A pre-processing phase on the paths collected by the optoelectronic system was required in order to remove the outliers, fill in the missing data and smooth the curves, and the path of each marker was interpolated with a smoothing spline. Then, considering the triangle that the three markers form (see againFig. 1), the path of a unique "virtual" marker

representing the human walking path was computed as the barycentre of the triangle.

III. INVERSE OPTIMAL CONTROL

In this section we describe the model used for the inverse optimal control, and the approach developed to solve it.

A. The unicycle model

As far as human trajectory planning is concerned, the complex activities performed during walking by muscles and brain in commanding and coordinating many elementary motor acts can be neglected, and the problem may be considered from a high-level kinematic perspective.

A walking human can be thus represented by the center of gravity of the body, that can translate and rotate with respect to the direction of the forward walking. The pose of the human is thus completely described by the 2D coordinates of the center of gravity, and by the angle θ formed by the tangent to the walking path with the x-axis.

The simplest kinematic model that can be used is the unicycle model

$$\begin{cases} \dot{x}_1 = u_1 \cos(x_3) \\ \dot{x}_2 = u_1 \sin(x_3) \\ \dot{x}_3 = u_2 \end{cases} \tag{1}$$

where x_1 and x_2 are respectively the x- and the y-coordinate of the center of gravity, x_3 is the orientation θ, u_1 is the linear (nonholonomic) velocity along the direction of motion, and u_2 is the angular velocity.

In order to apply optimal control techniques on this model, a discrete version is adopted. In the following we consider the Explicit Euler discretization method, i.e.,

$$\begin{cases} x_1(k+1) = x_1(k) + \tau u_1(k) \cos(x_3(k)) \\ x_2(k+1) = x_2(k) + \tau u_1(k) \sin(x_3(k)) \\ x_3(k+1) = x_3(k) + \tau u_2(k) \end{cases}, \tag{2}$$

where τ is the sampling time, and k is the discrete-time index.

B. Problem formulation

The inverse optimal control problem solved in [8] is

$$\begin{aligned} \min_{\mathbf{x}(k),\mathbf{u}(k)} \quad & \frac{1}{2}\tau \sum_{k=0}^{N-1} \left(c\left(u_1(k)\right)^2 + u_2(k)^2 \right) \\ \text{s.t.} \quad & \mathbf{x}(0) - \mathbf{x}_{\text{init}} = 0, \\ & \mathbf{x}(N-1) - \mathbf{x}_{\text{goal}} = 0, \\ & x_1(k+1) - [x_1(k) + \tau u_1(k) \cos(x_3(k))] = 0, \\ & x_2(k+1) - [x_2(k) + \tau u_1(k) \sin(x_3(k))] = 0, \\ & x_3(k+1) - [x_3(k) + \tau u_2(k)] = 0, \\ & \forall k = 0, \dots, N-1. \end{aligned} \tag{3}$$

where $\mathbf{x} = \begin{bmatrix} x_1 & x_2 & x_3 \end{bmatrix}^T$ is the state vector, $\mathbf{x}_{\text{init}}$ and $\mathbf{x}_{\text{goal}}$ are the initial and the final states, respectively, and N is the number of samples. The only unknown parameter is c, that governs how much u_1 is penalized with respect to u_2 in the minimization of the cost function. The considered cost function is related to the energy needed to perform the trajectory.

Solving the inverse optimal control problem associated with (3) may take a lot of computational time, due to its nonlinearities, thus in [8] a more efficient solution, based on the KKT conditions for optimality, is proposed and here briefly presented.

1) Necessary condition for optimality: Let $\chi = \begin{bmatrix} \mathbf{x}^T & \mathbf{u}^T \end{bmatrix}^T$, $f(\chi;c) \in \mathbb{R}$ the cost function, and $g(\chi) \in \mathbb{R}^m$ the set of constraints.

For a given c, assuming that $\chi^\star$ is a local minimum of the problem (3) and is regular, there exist unique Lagrange multiplier vectors $\lambda^\star \in \mathbb{R}^m$ [9] such that

$$\begin{cases} \nabla_\chi f(\chi^\star;c) + \sum_{i=1}^m \lambda_i^{\star T} \nabla_\chi g_i(\chi^\star) = 0 \\ g(\chi^\star) = 0 \end{cases} \quad (4)$$

assuming that $f(\cdot)$ and $g(\cdot)$ are continuously differentiable functions. Equations in (4) are known as the KKT necessary (and sufficient) conditions for equality constraint optimization problems: the first one is the stationarity condition, while the second equation ensures primal feasibility.

Thus, the KKT conditions for the Lagrangian of problem (3) can be written as

$$\nabla_{(\chi,\lambda)} \mathscr{L}(\chi,c,\lambda) = \nabla_{(\chi,\lambda)} \left(f(\chi;c) + \sum_{i=1}^m \lambda_i^T g_i(\chi) \right) = 0.$$

2) Residual functions: As previously stated, the system is assumed to be only "approximately optimal", while observations are assumed to be perfect. In [8], the inverse optimal control problem is solved by minimizing the residual function

$$\min_{c,\lambda} \quad \frac{1}{2} \|\nabla_{(\chi,\lambda)} \mathscr{L}(\chi,c,\lambda)\|^2 = \min_{c,\lambda} \quad \frac{1}{2} \|Jz - b\|^2, \quad (5)$$

where $z = \begin{bmatrix} c & \lambda \end{bmatrix}^T$, while J and b depend on the collected data.

One can see that the initial constrained optimization problem (3) has been cast into the unconstrained optimization problem (5), with the only limitation that the objective function needs to be composed of a linear combination of known basis functions. The problem therefore becomes a convex unconstrained least-squares optimization, which is easier to solve than the initial constrained optimization one, and reads as the classical normal equation, i.e., with the solution $z^\star = J^\dagger b$, where $J^\dagger$ denotes the Moore-Penrose pseudoinverse of J.

3) Limits of the approach: One of the main limitations of the approach formulated in [8] is that there is no guarantee that the value of $c^\star$ resulting from the normal equation is actually positive. In fact, in many cases, starting from the considered dataset, the solution is a negative value of c, making the optimization problem not convex (the cost function in (3) becomes a saddle).
To overcome this problem, the solution of the normal equation is here taken as the initial guess for the solution of a new optimization problem, i.e., a constrained version of (5), which reads as

$$\min_{c,\lambda} \quad \frac{1}{2} \|Jz - b\|^2$$
$$\text{s.t.} \quad c \geq 0.$$

Therefore, for each trajectory in the database the optimum value $c^\star$ was computed, obtaining an average value $\bar{c} = 0.0595$. Using $\bar{c}$ to solve (3) yields unsatisfactory results. Just to give an example, let's consider a particular trajectory (see Fig. 4) in which apparently the solution of the optimization problem (the blue line) is not able to reproduce reliably the collected data (the black line). This issue arises in many other optimized trajectories, omitted here for space limitations.
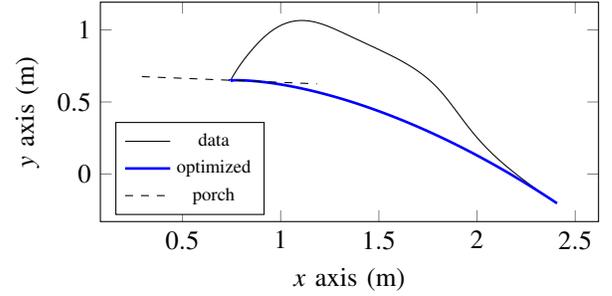

Fig. 4: Solution of the optimization problem.

It is opinion of the authors that this kind of issue in reproducing the collected data is not only due to the fact that the chosen value of c is not the optimal one – in fact, even the optimal ones produce similar results –, but also to the selected cost function, which is inherently not able to replicate the human way of planning trajectories. This is also revealed by the fact that in many the cases, even if the geometry of the trajectory is close to the data, the computed values of u_1 and u_2 are really different from the ones measured during the experiments (see Fig. 5). In particular, u_1 tends to be unrealistic (if compared with
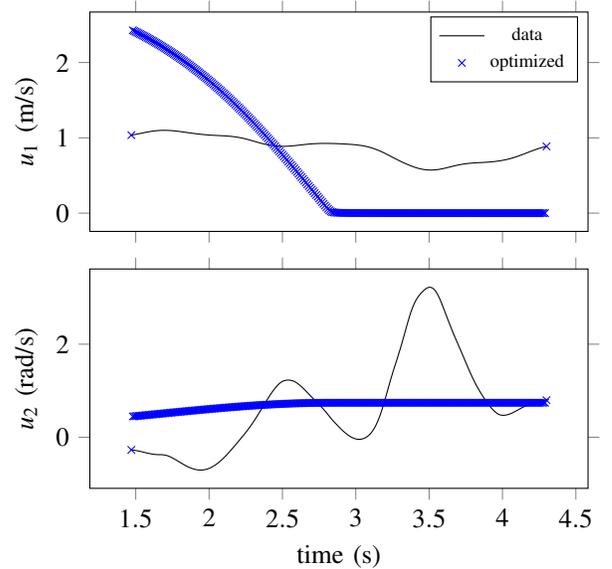

Fig. 5: Inputs of the unicycle model.

the human velocity), and, in the authors' opinion, it is not relevant to understand how humans plan the paths. Thus, in the following we modify the cost function (and the model) accordingly.

C. The model in the natural coordinate

If one is interested in studying the geometry of the walking path only, instead of the complete trajectory as a function of time, it is possible to rewrite model (1) with the natural coordinate s as the independent variable, making the model invariant with respect to changes in the velocity u_1, and reducing the number of input variables. Thus, if $u_1 > 0$ along the path (which is one of the assumptions of this work) the relation between the natural coordinate s and the time t is given by $s(t) = \int_0^t u_1(\tau)\,d\tau$, and can be inverted defining $t = t(s)$. As a consequence, defining $x' = dx/ds$, the unicycle model (1) as a function of space can be written as

$$\begin{cases} x_1'(s) = \cos(x_3(s)) \\ x_2'(s) = \sin(x_3(s)) \\ x_3'(s) = u_2(s) \end{cases} \tag{6}$$

where $u_2(s)$ is the angular velocity with respect to s. Model (6) can be discretized yielding

$$\begin{cases} x_1(k+1) = x_1(k) + \sigma(k)\cos(x_3(k)) \\ x_2(k+1) = x_2(k) + \sigma(k)\sin(x_3(k)) \\ x_3(k+1) = x_3(k) + \sigma(k)u_2(k) \end{cases} \tag{7}$$

where $\sigma(k) = s(k) - s(k-1)$, and, now, k is not a time, but a space index.

In order to understand whether this model is suited for our purposes, we compared simulation results with the collected data (see Fig. 6), obtaining a very good match.
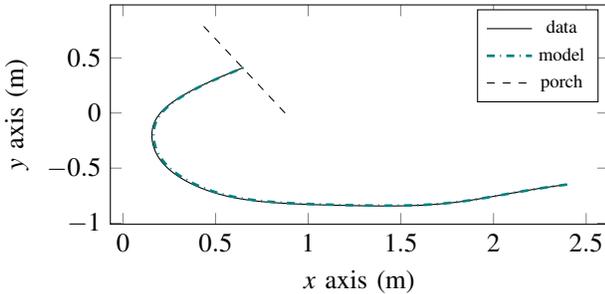

Fig. 6: One of the trajectories used for validating the model.

D. The proposed cost function

In this section we propose a new cost function, the parameters of which are identified with the same procedure presented in Section III-B.

The proposed cost function accounts for the energy related to the angular velocity u_2, and for the distance between the current state and the final state, i.e.,

$$f(\mathbf{x}, u_2; \mathbf{c}) = \frac{1}{2}\sum_{k=0}^{N-1} \sigma(k)\,(u_2(k))^2 \cdot \left(1 + \mathbf{c}^T \delta\mathbf{x}^2\right), \tag{8}$$

where

$$\mathbf{c} = \begin{bmatrix} c_1 \\ c_2 \\ c_3 \end{bmatrix}, \qquad \delta\mathbf{x}^2 = \begin{bmatrix} \left(x_1(k) - x_{1,\text{goal}}\right)^2 \\ \left(x_2(k) - x_{2,\text{goal}}\right)^2 \\ \left(x_3(k) - x_{3,\text{goal}}\right)^2 \end{bmatrix}.$$

The assumption here is that the distances of the current state from the goal values can be interpreted as space- (time-) varying weights on the angular velocity u_2, and then chosen as the terms to be weighted.

Therefore, we can write the new optimization problem as

$$\begin{aligned} \min_{\mathbf{x}(k), u_2(k)} \quad & \frac{1}{2}\sum_{k=0}^{N-1} \sigma(k)\,(u_2(k))^2 \cdot \left(1 + \mathbf{c}^T\delta\mathbf{x}^2\right) \\ \text{s.y.} \quad & \mathbf{x}(0) - \mathbf{x}_{\text{init}} = 0, \\ & \mathbf{x}(N-1) - \mathbf{x}_{\text{goal}} = 0, \\ & x_1(k+1) - [x_1(k) + \sigma(k)\cos(x_3(k))] = 0, \\ & x_2(k+1) - [x_2(k) + \sigma(k)\sin(x_3(k))] = 0, \\ & x_3(k+1) - [x_3(k) + \sigma(k)u_2(k)] = 0, \\ & \forall k = 0, \dots, N-1, \end{aligned} \tag{9}$$

and, writing the Lagrangian associated with (9) as described in Section III-B.1, the residual functions matrices of (5) become

$$z = \begin{bmatrix} \mathbf{c}^T & \lambda_1^0 & \lambda_2^0 & \lambda_3^0 & \cdots & \lambda_1^{N-1} & \lambda_2^{N-1} & \lambda_3^{N-1} \end{bmatrix}^T,$$

$$b = \begin{bmatrix} \zeta(0)^T & \zeta(1)^T & \cdots & \zeta(N-1)^T \end{bmatrix}^T,$$

and

$$J = \begin{bmatrix} \psi(0) & I_{4\times3} & M(0) & \mathbf{0}_{4\times3} & \cdots & \mathbf{0}_{4\times3} \\ \psi(1) & \mathbf{0}_{4\times3} & -I_{4\times3} & M(1) & \cdots & \mathbf{0}_{4\times3} \\ \psi(2) & \mathbf{0}_{4\times3} & \mathbf{0}_{4\times3} & -I_{4\times3} & \cdots & \mathbf{0}_{4\times3} \\ \vdots & \vdots & \vdots & \vdots & \ddots & \vdots \\ \psi(N-1) & \mathbf{0}_{4\times3} & \mathbf{0}_{4\times3} & \mathbf{0}_{4\times3} & \cdots & -I_{4\times3} \end{bmatrix}$$

with

$$\zeta(k) = \begin{bmatrix} 0 \\ 0 \\ 0 \\ \sigma(k)u_2(k) \end{bmatrix}, \qquad I_{4\times3} = \begin{bmatrix} I_{3\times3} \\ \mathbf{0}_{1\times3} \end{bmatrix},$$

$$\psi(k) = \sigma(k)u_2(k) \cdot$$
$$\begin{bmatrix} u_2(k)\delta x_1(k) & 0 & 0 \\ 0 & u_2(k)\delta x_2(k) & 0 \\ 0 & 0 & u_2(k)\delta x_3(k) \\ \delta x_1(k)^2 & \delta x_2(k)^2 & \delta x_3(k)^2 \end{bmatrix},$$

$$M(k) = \begin{bmatrix} 1 & 0 & 0 \\ 0 & 1 & 1 \\ -\sigma(k)\sin(x_3(k)) & \sigma(k)\cos(x_3(k)) & 1 \\ 0 & 0 & \sigma(k) \end{bmatrix}.$$

Even in this case, it is possible to find a solution to the normal equation, and determining the values of $\mathbf{c}$ in a very efficient way. However, it is not possible to guarantee that $\mathbf{c} \geq 0$, thus the solution $z^\star$ of the normal equation is used as the initial guess for the constrained problem

$$\begin{aligned} \min_{c, \lambda} \quad & \frac{1}{2}\|r(\chi, c, \lambda)\|^2 \\ \text{s.t.} \quad & \mathbf{c} \geq 0. \end{aligned} \tag{10}$$

The average weights obtained using the collected data are $\bar{\mathbf{c}} = \begin{bmatrix} 125.1760 & 42.4662 & 189.8515 \end{bmatrix}^T$, values that are used for the solution of the optimization problem (9).

Even if the choice of the weights could not be the optimal one, the obtained results are really encouraging. Recalling

the trajectory example presented in Section III-B.3 (Fig. 4, top) the previous approach was not able to reproduce the human trajectory, leading to a solution of the optimization problem that was not even passing through the porch. In this case, the solution not only passes through the porch, but also its shape is very similar to the actual human path (see Fig. 7, bottom).
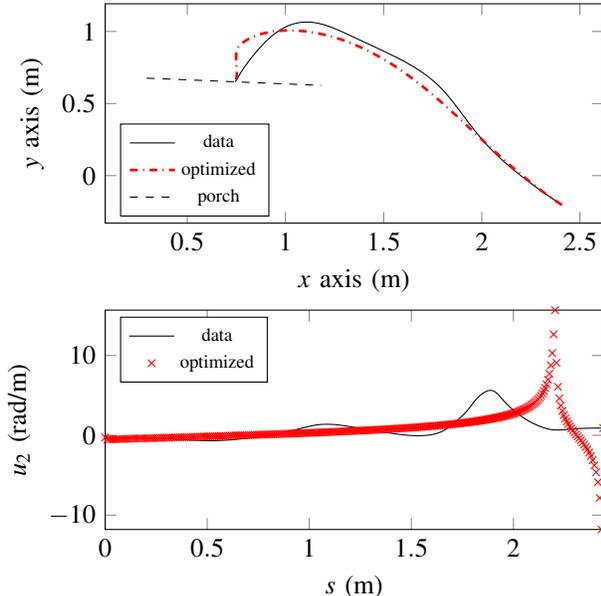

Fig. 7: Solution of the optimization problem with the proposed approach.

On the other hand, however, the computed u_2 does not fit exactly the actual angular velocity obtained from the data, showing a peak while the porch is almost reached (see Fig. 7). Anyway, the overall trend is caught, and can be considered as an average of the actual input.

This result could be improved, for example, by accounting in the cost function the first and second derivative of u_2 as well, introducing some inertia in the curvature and thus avoiding discontinuities in the input.

Notice that the chosen human path is deliberately one of the most difficult to reproduce, due to its curvature and final orientation. In other cases the results that can be obtained with the presented approach are even better, as it will be shown in the next section.

IV. EXPERIMENTAL RESULTS AND DISCUSSION

In this section the results obtained with the presented approaches are analysed in more details. In particular, more experimental results are presented, and a way to evaluate the distance between the obtained curves and the human paths is described, i.e., the Fréchet distance [10].

A. Experimental results

For the sake of clarity, we refer to the first method presented in Section III-B as the *Time method*, and to the second one presented in Section III-D as the *Space method*, with obvious meanings. The solution of the nonlinear optimization problems (3) and (9) is performed using an interior point algorithm [9].

Fig. 8 shows a sample of representative trajectories. The black solid lines are the data collected from the human trajectories, the blue dashed lines the solutions of the time method, while the red dash-dotted lines are the solutions of the space method.

Apparently, in some cases both the methods manage to reproduce the human trajectory, but also in those cases, the space methods *seems* to be *closer*. In several other cases, however, the time method definitely fails. From a qualitative point of view, it is already clear that the novel approach overcomes the limitations of the time method highlighted in Section III-B.3, but the performance of both methodology from a quantitative viewpoint needs discussing.

B. Discussion

To evaluate the performance of the approaches, we need to quantify *how far* the obtained solution (with any method) is from the collected data. The classical way to quantify the distance between two curves is the ℓ^2-norm (Euclidean distance) [5], [11]–[13]. In the opinion of the authors, this is not the most suited distance to compare the shape of two paths.

A different way to measure the distance between two curves is here proposed, i.e., the Fréchet distance [10], which is particularly used in computational geometry as a "similarity" metric between two curves.

Formally, the Fréchet distance is defined as follows. Given two curves $f : [a,b] \to V$ and $g : [a',b'] \to V$, their Fréchet distance is defined as

$$\delta_F(f,g) = \inf_{\alpha,\beta} \max_{t \in [0,1]} \quad d\left(f\left(\alpha\left(t\right)\right), g\left(\beta\left(t\right)\right)\right)$$

where α and β are arbitrary continuous non-decreasing function from $[0,1]$ onto $[a,b]$ and $[a',b']$ respectively. In computing the Fréchet distance between arbitrary curves one typically approximates the curves f and g by polygonal curves f_N and g_M of N and M points respectively, and uses the discrete Fréchet distance $\delta_{dF}(f_N,g_M)$.

Hence, the discrete Fréchet distance was computed for all the paths computed by the two methods with respect to the human ones. Fig. 9 shows the boxplot of the obtained distances.

The red crosses in the boxplot represent the outliers, while the red dots are the computed average (also considering the outliers). Statistical properties of the obtained discrete Fréchet distances are presented in Table I. As it might be

TABLE I: Statistical properties of δ_{dF}.

Method	Avg (m)	Var (m^2)	Min (m)	Max (m)	Med (m)
Time	0.2840	0.0738	0.0016	1.1084	0.1525
Space	0.0833	0.0057	0.0029	0.5642	0.0640

expected from the qualitative considerations of Section IV-A, the proposed method gives better results with respect to the time method.

V. CONCLUSION AND FUTURE WORK

In this work, we dealt with the problem of identifying how humans plan their paths, modelling this problem as an inverse optimal control one.
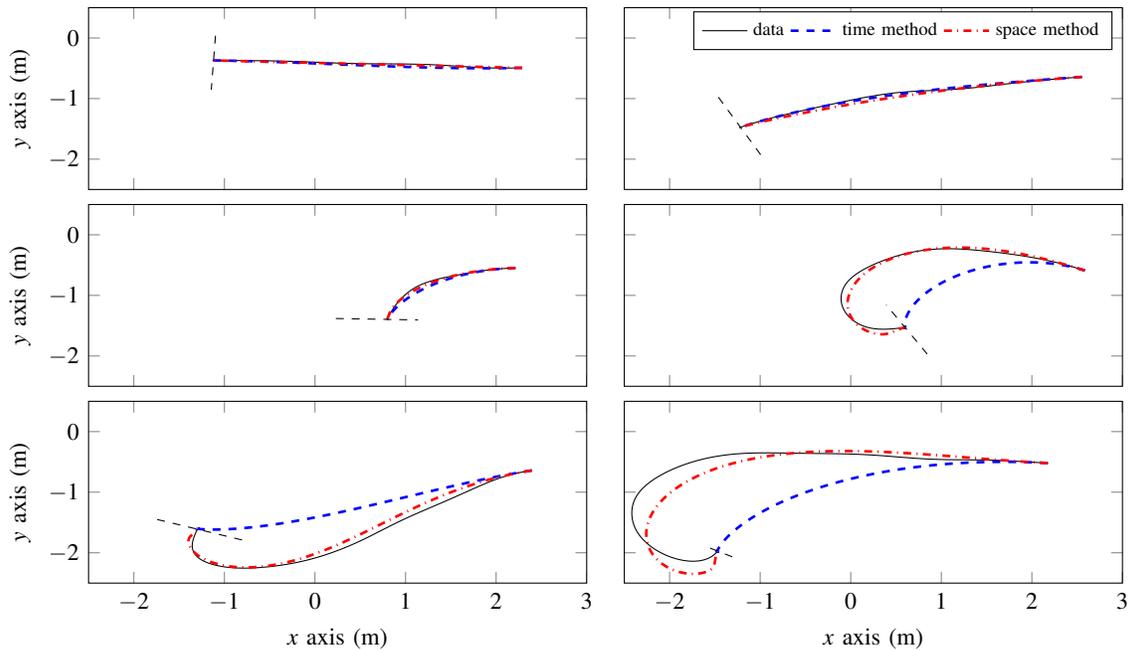
Fig. 8: A representative sample of paths. The trajectories start from the same initial condition, while the black dashed line represents the porch width (final configuration).
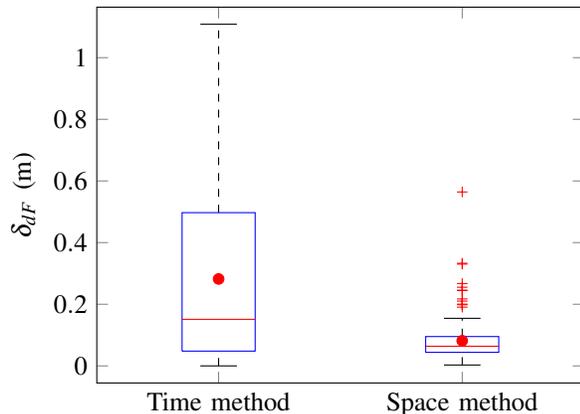

Fig. 9: Boxplot of the computed discrete Fréchet distances.

To this end, experiments on volunteer subjects were conducted, and a modified version of a promising and recent approach [8] was used to solve the problem. It was then compared with a novel one, able to overcome the highlighted former limitations. The results were evaluated with the discrete Fréchet distance, a metric that was never used for the performance measurement in the context of generation of human walking paths to date.

Starting from this work, different research directions can be identified. For example, terms can be added to the cost function, accounting for the inertia of changing the orientation, i.e., inertia on u_2, improving the prediction capabilities of the proposed method.

ACKNOWLEDGEMENT

REFERENCES

[1] L. Bascetta, G. Ferretti, P. Rocco, H. Ardo, H. Bruyninckx, E. Demeester, and E. Di Lello, "Towards safe human-robot interaction in robotic cells: an approach based on visual tracking and intention estimation," in *IEEE/RSJ Int. Conf. on Intelligent Robots and Systems*, 2011, pp. 2971–2978.

[2] K. Mombaur, A. Truong, and J.-P. Laumond, "From human to humanoid locomotion–an inverse optimal control approach," *Autonomous Robots*, vol. 28, pp. 369–383, 2010.

[3] A. Jameson and E. Kreindler, "Inverse problem of linear optimal control," *SIAM Journal on Control*, vol. 11, no. 1, pp. 1–19, 1973.

[4] J. Casti, "On the general inverse problem of optimal control theory," *J. Optimization Theory and Applications*, vol. 32, pp. 491–497, 1980.

[5] G. Arechavaleta, J.-P. Laumond, H. Hicheur, and A. Berthoz, "An optimality principle governing human walking," *IEEE Transactions on Robotics*, vol. 24, no. 1, pp. 5–14, Feb. 2008.

[6] K. Dvijotham and E. Todorov, "Inverse optimal control with linearly-solvable MDPs," in *Interntional Conference on Machine Learning*, 2010.

[7] A. Keshavarz, Y. Wang, and S. Boyd, "Imputing a convex objective function," in *IEEE Int. Symposium on Intelligent Control*, 2011, pp. 613–619.

[8] A.-S. Puydupin-Jamin, M. Johnson, and T. Bretl, "A convex approach to inverse optimal control and its application to modeling human locomotion," in *IEEE Int. Conf. on Robotics and Automation*, 2012, pp. 531–536.

[9] D. Luenberger and Y. Ye, *Linear and nonlinear programming*. Springer, 2008, vol. 116.

[10] H. Alt and M. Godau, "Computing the fréchet distance between two polygonal curves," *Int. Journal of Computational Geometry & Applications*, vol. 5, no. 1 & 2, pp. 75–91, 1995.

[11] G. Arechavaleta, J.-P. Laumond, H. Hicheur, and A. Berthoz, "Optimizing principles underlying the shape of trajectories in goal oriented locomotion for humans," in *IEEE/RAS Int. Humanoid Robots Conference*, 2006, pp. 131–136.

[12] ——, "The nonholonomic nature of human locomotion: a modeling study," in *IEEE/RAS-EMBS Int. Conf. on Biomedical Robotics and Biomechatronics*, 2006, pp. 158–163.

[13] K. Mombaur, J.-P. Laumond, and E. Yoshida, "An optimal control model unifying holonomic and nonholonomic walking," in *IEEE/RAS Int. Conf. on Humanoid Robots*, Dec. 1–3, 2008, pp. 646–653.